PART 1.

Setting The Scene

1

Observations of Disks and Outflows from Young Stars

John Bally[1]

Campus Box 389, Center for Astrophysics and Space Astronomy,
University of Colorado, Boulder CO 80309, USA

Abstract. I review recent observations and accretions disks and jets powered by young stellar objects.

1. Introduction

The disks and jets associated with young stellar objects (YSOs) represent one of the most common examples of accretion phenomena in astrophysics. Stars form in the Galaxy at a rate of about 1 to 3 $M_\odot$ yr^{-1}. The median mass of stars is about 0.5 $M_\odot$, so about 2 to 10 stars are born each year on average. The bulk of accretion onto a YSO occurs from a surrounding disk and lasts about 10^5 years. During this phase, young stars drive powerful jets and bipolar outflows into the surrounding medium. At any one time, there must be between 10^5 to 10^6 active accretion disk/jet systems in the Milky Way which we can study. Since all stars went through such a phase during their formation, they represent the largest category of observable objects formed by accretion in the Universe.

Stars are born in the dense cores of 10^4 to 10^6 $M_\odot$ giant molecular clouds (GMCs). The total mass of molecular gas in the Galaxy is about 2 to 4 $\times 10^9$ $M_\odot$ and there is a comparable amount of atomic hydrogen (HI). Thus, the total reservoir of interstellar gas that is available for star formation is about 4 to 8 $\times 10^9$ $M_\odot$, a few percent of the baryonic mass of the Milky Way.

Millimeter wavelength observations of nearby GMCs show that the cloud cores in which stars form range from 1 to more than 1000 $M_\odot$. GMCs are supported against global gravitational collapse by magnetic fields and MHD turbulence. Gravitational collapse of molecular cloud cores can occur via two distinct modes (see Shu et al. 1993 and refenences therein). *Magnetic supercritical collapse* occurs when a sufficient density of material accumulates in a given region so that the inward pull of gravity overwhelms the outward pressure of magnetic fields. For mean GMC parameters near the Sun, this tends to occur on mass scales of order 10^3 $M_\odot$. Further fragmentation may lead to the formation of dense clusters of stars on a collapse time scale. Collapse can also occur more slowly via *ambipolar diffusion* as neutrals slip through the magnetic field and the ions and electrons coupled to it, lowering the mass where gravitational collapse overwhelms pressure support to about 1 $M_\odot$.

---

[1]Center for Astrophysics and Space Astronomy

Most star-forming cores produce ultra-dense but *transient clusters* of stars (Lada et al. 1991a,b; Lada, Strom, & Myers 1993). Although some star formation occurs in isolated small clouds and globules which may have collapsed through ambipolar diffusion or by external compression, isolated star formation is relatively rare in the Solar vicinity (Reipurth 1983). Out of the approximately 10^4 to 10^5 stars formed in the past 10^7 years within a distance of 500 pc from the Sun, most were formed in transient clusters in the major OB associations (Orion OB1, Perseus OB2, and the Sco-Cen OB Association). In Orion, most of the young stars are concentrated into 7 to 8 clusters containing between 50 and 700 stars each typically in a volume much smaller than a cubic parsec. Even in the dark clouds however, star formation is highly clustered. In the L1551 core in Taurus, over a dozen stars were born in the past 10^6 years in a region that has a diameter of only several tenths of a parsec.

Such star clusters usually dissolve in less than 10^6 years because the efficiency of star formation (mass of stars formed / initial available mass of gas) is on average 5 to 15%. Young stars typically move with a random velocity close to the initial escape velocity from a cloud core, and if more than 70% of the initial gas mass is removed by ionization or the impact of stellar outflows, the resulting cluster will disperse.

Stellar-mass fragments in gravitationally collapsing GMC cores typically develop specific angular momenta (angular momentum per unit mass) about 5 orders of magnitude larger than that of stars through mutual tidal interactions between adjacent cores or by other differential forcing. Rotating cores collapse into disks, which through dissipation of their angular momentum, probably mediated by magnetic fields, accrete onto a central proto-star. Magnetic fields in the collapsing, rotating cloud cores are advected with the accretion flow to form an hour-glass shaped and twisted B-field that is pinched inward by the disk. Soon after its formation, the proto-star becomes fully convective and supports a rigid, co-rotating (with the star), roughly di-polar stellar B-field which may extend outwards for up to 5 or 10 stellar radii. The point where the outermost stellar field line intersects the accretion disk determines the rotation rate of the young star. This point will rotate with the Keplerian rotation speed of the disk at that radius. Matter is picked up from the disk, forced to move along magnetically dominated accretion columns to high stellar latitudes, where it is accreted onto the star. Most workers have adopted some variant of this magnetic geometry, first worked out by Ghosh & Lamb (1977, 1978). The magnetic X point where the stellar field intersects the disk is the point of origin of a magnetocentrifugally driven wind fueled by matter injected onto open field lines and flung to infinity (Lovelace et al. 1995; Wardle & Königl 1993; Shu et al. 1994; Ostriker & Shu 1995). Magnetic forces ("hoop stress") on the open field lines 0.1 to 10 AU from the central star are responsible for collimating the wind into a stellar jet. Observations make it clear that stellar accretion and mass loss from the young star or its disk are highly variable. Models to date have not incorporated the full range of possible time-dependent behaviors expected of such a system.

What removes most of the initial mass of gas in a core and brings star formation to a halt? If massive stars are formed, UV radiation, stellar winds, and supernova explosions dissociate, ionize, heat, and accelerate the remaining gas to speeds in excess of the escape velocity from the region. When only low

mass stars form, residual gas may be dispersed by the impact of mass outflows and jets.

2. Externally Illuminated Accretion and Proto-Planetary Disks

Evidence for accretion disks surrounding YSOs comes from the infrared excess and IR spectra, from the large column of dust detected at mm and sub-mm wavelengths combined with low extinction towards the star, and from direct imaging of the gas and dust with interferometers. The most compelling and highest angular resolution observations of disks come from Hubble Space Telescope (HST) which provides angular resolution better than 0.05″.

Proto-planetary disks surrounding young stars embedded in the Orion Nebula were discovered in the seminal observations of C. R. O'Dell and collaborators (O'Dell et al. 1993; O'Dell & Wen 1994). We have used the PC portion of WFPC2 to obtain 0.05″ images in the visible, FOC to push the angular resolution close to 0.02″ on a few objects, and FOS to obtain the first UV spectra.

The Trapezium region in the Orion nebula contains about 700 stars with a core density of 5×10^5 stars per cubic parsec (McCaughrean & Stauffer 1994). More than half are now embedded in the H II region ionized by the O6p star θ^1C Orionis which drives a powerful isotropic stellar wind with a mass loss rate of about $\dot{M} = 10^{-7}$ M$_\odot$ yr^{-1} at a wind velocity that has been estimated to lie between 500 and 1500 km s^{-1}. Young low-mass stars have been exposed to an intense radiation field, and for stars lying within the stellar wind cavity, also to a massive stellar wind. Herbig & Terndrup (1986) found that the median age of stars in the Trapezium cluster is only about 3×10^5 years. Many have retained a portion of their circumstellar environments. Photo-ablation of the low density envelope surrounding a YSO embedded inside an HII region removes the obscuring material that normally hides the accretion disk. External illumination by nearby massive stars, or back-lighting by the ionized gas, permits us to study the structure of such disks with the unprecedented angular and linear resolution of HST ($< 0.03''$ or 15 AU in Orion) at UV and visual wavelengths.

At least 150 stars in the inner region of the Orion Nebula contain extended circumstellar environments. Consideration of the physical processes involved indicates a sequence of expected morphologies with increasing distance from θ^1C Ori. Stars lying within the inner stellar wind bubble are first exposed to ionizing UV. The gas that is evaporated from the YSO circumstellar environment expands at approximately the sound speed in ionized gas and shocks against the stellar wind. Young stellar objects within 30″ of the hottest star in the Trapezium (θ^1C Ori) have arcs of [O III] and Hα emitting gas several arc seconds from the YSO. Ground based spectra show that at least some of these arcs are associated with high radial velocity gas, consistent with the wind shock model. Soft non-ionizing UV can penetrate the ionization front on the side of the YSO environment that faces θ^1C Ori. The radiation can couple strongly to the grains, dragging them through the gas, effectively straining (removing dust from) the gas that expands through the ionization front. The dust is driven radially away from the hot star, forming the spectacular cometary tails seen in the objects near the Trapezium (see first panel in Figure 1). From the surface brightness of the ionization front and the radio free-free flux, it is estimated that the typical
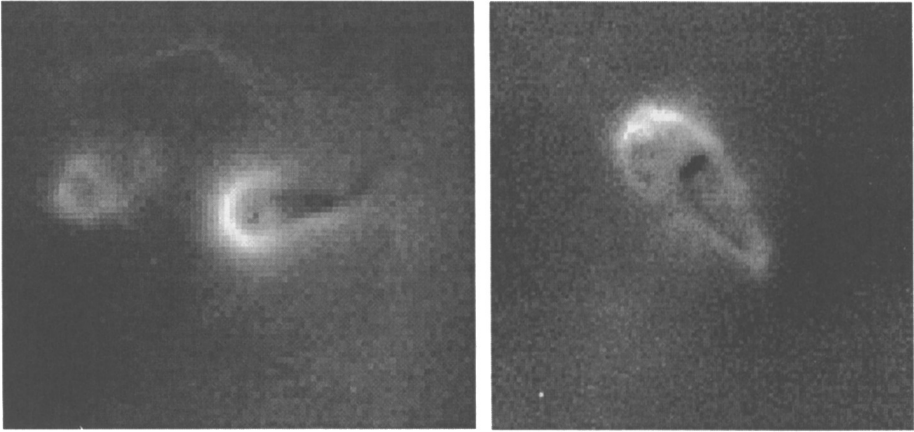
Figure 1.   (**left**): An [O III] image showing the objects LV6 (HST4, 158-327) and LV6N (158-326) to the left, located about 15″ to the southwest of θ^1C Ori. Note the central star, and ring of absorption that surrounds it, in the more prominent object. North is toward the upper left in all images and θ^1C Ori is located to the lower left in this image. (**right**): HST10 (182-413) has an opaque and edge-on central disk embedded in a bright teardrop-shaped ionization front in Hα. θ^1C Ori is located about 50″ above. Both images were obtained with the 0.05″ (25 AU) resolution of the Planetary Camera on Hubble Space Telescope with narrow band filters.

mass loss rate of each YSO environment is about 10^{-7} M$_\odot$ yr^{-1} so that if the environment contains 0.01 M$_\odot$, it can survive for about 10^5 years.

For YSOs located outside the ram pressure (n_{wind} proportional to r^{-2}) dominated portion of the stellar wind bubble, the [O III] arcs disappear. Since the intensity of radiation diminishes with increasing distance from the Trapezium, dust tail production also becomes less significant, and the ionization fronts that form around these young stars take on a tear-drop shape determined by the ratio of direct to scattered nebular UV ionizing continuum (second panel showing HST 10 in Figure 1). Circumstellar disks present inside the photo-ionization fronts surrounding the young stars produce silhouettes against the background nebular light (cf. HST10 in Figure 1). Silhouettes are seen in the cometary objects near the Trapezium, the teardrop shaped objects located far from the Trapezium but still within the photoionized nebula, and in YSOs completely outside the Orion Nebula's Strömgren sphere, where no ionizing radiation can penetrate and no ionization fronts are produced (see Figure 2). At least 6 dark silhouettes which are not surrounded by ionization fronts have been found (McCaughrean & O'Dell 1996).

3.   The Jets of Herbig and Haro

Herbig-Haro (HH) objects are collisionally excited nebulae powered by jets and outflows from young stars (Schwartz 1975; Raymond 1979). Today, well over 300

Figure 2.   A large edge-on disk (114-426) seen in silhouette against the bright background of the Orion Nebula in the red 6584Å line of [N II]. This object lies at a projected distance of 90″ from θ^1C Ori and appears to be surrounded on one side by a shock-heated bubble that may be a Herbig-Haro object produced by a wind from a star hidden in the disk. A faint cone of [N II] emission connects the disk to a bright spot in the bubble and may be a jet. This image was obtained with the WFPC3 camera on HST with a scale of 0.1″ (50 AU) per pixel.

individual HH objects or groups are known (Reipurth 1994). Many individual HH objects consist of separate knots or bow shocks, others consist of highly linear chains or jets. Most show evidence of being a part of or excited by a highly collimated flow from a young star. Millimeter wavelength observations of carbon monoxide (CO) frequently reveal bi-directional, axially symmetric, but poorly collimated *molecular outflows*, of moderate velocity (3 to 100 km s^{-1}) CO bearing gas (Lada 1985; Fukui et al. 1993). We now believe that HH objects and CO outflows are different manifestations of the mass loss produced during star formation (Masson & Chernin 1993; Raga & Cabrit 1993).

Most CO outflows, when inspected with sufficient sensitivity, are found to contain HH objects or shock-excited near-infrared emission lines. Observations and models indicate that the high velocity jets ejected by young stars are the source of energy for HH objects with increasingly complex morphologies farther from their central sources. When such jets interact with molecular gas in their surroundings, they accelerate CO bearing gas. In some cases, the high pressure post-shock cooling layers can be sufficiently dense so that molecule formation time-scales are comparable to dynamic time scales. Under such conditions, which are found close to the driving sources of the youngest stars where internal working surfaces are formed by the interaction of faster jet fluid elements moving into slower fluid elements, clumps of very high velocity molecules can

be formed. These may be the so called molecular "bullets" observed in jet-like molecular outflows such as L1448C, IRAS03282, and HH 111 (cf. Cernicharo & Reipurth 1996).

It is apparent that outflows from young stellar objects are an integral part of the star formation process. Most stars undergo a phase that lasts for over 10^5 years during which energetic mass loss occurs in the form of numerous eruptions. Jets have ejection velocities of order several hundred kilometers per second for low mass stars, and in excess of 10^3 km s^{-1} for high luminosity sources that will evolve into O, B, and A stars. Jet densities range from n = 10^2 to over 10^5 cm^{-3}, and the ionization fractions vary from way below 1% to 10%. The shock cooling times are short (few to thousands of years), which lead to a very rich variety of structures resulting from a combination of cooling and hydrodynamic instabilities (Visniak and Rayleigh-Taylor instabilities; see Stone et al. 1995) and time dependent variations in the outflow parameters. The multiple bow shocks and S-shaped point symmetry seen in some sources almost certainly requires variations in the mass ejection velocity to produce internal working surfaces and precession or irregular wobbling of the jet.

Many stellar jets are sufficiently close to measure proper motions, the structure of components with high angular resolution, and their time dependent behavior. This is the only category of supersonic astrophysical jet where we can measure 5 out of the 6 phase-space dimensions!

Protostellar jets appear to evolve into parsec scale outflows which may dominate the injection of kinetic energy, dissociation of molecular gas, and generation of supersonic turbulence in GMCs in portions of the cloud where only low to intermediate mass stars are forming.

3.1.   The HH 34 System

The first parsec-scale Herbig-Haro flow was discovered in 1993 (Bally & Devine 1994) with the 23′ FOV of the KPNO 0.9-m telescope. The HH 34 (Reipurth et al. 1986) system in the Orion A molecular cloud consists of a 20′ long chain of HH objects, which corresponds to a projected length of 3 parsecs at a distance of 500 pc. The entire chain of HH objects appear to be energized by the one YSO that powers the HH 34 jet.

The lower left panel of Figure 3 shows a narrow band image (in Hα + [S II]$\lambda\lambda$6716, 6731 emission) of the HH 34 jet obtained with the Hubble Space Telescope. The driving source is located to the upper right of the slender jet which consists of a chain of knots, which upon close inspection, are resolved into a train of bow shocks. Ground based spectra and proper motions show that the individual knots in the jet are moving away from the source at about 220 to 250 km s^{-1}, and the jet is inclined about 20° to 30° from the plane of the sky. The low-excitation emission indicates very low shock velocities ($<$ 50 km s^{-1}) in the knots, which must be internal working surfaces within the jet where slight flow velocity variations produce shocks. The jet fades about 30″ from the source. About 90″ south of the central star, there is a spectacular bow shock, HH 34, where the jet encounters much slower moving neutral material. The bow is bright in Hα and has [O III] emission at its apex, implying shock velocities around 150 km s^{-1}. The shock propagating back into the decelerating jet (the reverse shock) is bright in [S II] emission. Thus, the bow shock is

stronger (faster) than the reverse shock, indicating that the jet material is much denser than the medium into which it is moving. The bow-shock is corrugated and wavy, indicating that instabilities may be starting to develop or that the pre-shock medium is inhomogeneous.

HH 34 itself is the first in a chain of increasingly complex bow shocks lying to the south. Next in line are HH 34X, HH 172, HH 86, HH 87, and HH 88. Spectroscopy and proper motions show that all of these bow-shocks are moving to the south and are blue shifted. There is a systematic decrease in the amplitude of the velocity vector with increasing distance from the source. There is also a systematic increase in the degree of fragmentation and morphological complexity of the bow shocks with increasing age and distance from the source, indicating the growth of non-linear thermal or dynamic instabilities. To the north, there is a counter-chain of shocks, starting with HH 34N, and containing HH 126, HH 85, and ending in HH 33/40. All of these objects are moving approximately north and have redshifted velocities. Overall, the HH 34 system exhibits S-shaped point symmetry about the central source, indicating that over the 10^4 year life of the most distant HH objects, the ejection direction of the jet has precessed or wobbled by an angle of order 5° or 10°.

The HH 34 system is associated with a weak CO outflow (Chernin & Masson 1995) that is confined to the inner arc minute nearest the young star. We know from the low obscuration of the shocks in this system that this outflow must lie near the front face of the L1641 (Orion A) molecular cloud in the southern portion of the Orion OB association (Bally et al. 1987; Bally, Liu, & Langer 1991). The jet may be mostly ramming atomic gas, except in the immediate vicinity of the remnant cloud core that surrounds the HH 34 driving source.

3.2. Consequences of Parsec Scale Flows

Within the past two years, we have found over 2 dozen examples of parsec-scale outflows from regions of known star formation (Reipurth, Bally, & Devine 1997). Previous workers have missed the large angular scales of these outflow because they were using smaller format detectors, or did not map a sufficiently large region of the sky at IR or mm wavelengths.

Most parsec-scale flows consist of more or less regularly spaced HH objects, implying time-scales for major outbursts ranging from several hundred to over 10^3 years, roughly comparable to the intervals between FU Ori outbursts. Proper motions and radial velocities tend to decrease with increasing distance from the source stars. (cf. HH33/40/86/87/88 in the HH34 system and HH 311 and HH 113 driven by HH111). Many show S-shaped point symmetry about the central source. A typical dynamical age for a shock in a parsec-scale HH flow is $\tau_{dyn} = 10^4 \, d_{pc}/v_{100}$ years, where d is in parsecs and v_{100} is the apparent velocity in units of $100 km \, s^{-1}$. The dynamical ages of the outermost visible components range from 10^4 to 10^5 years. The longer time scale is comparable to the estimated duration of both the stellar accretion phase and the lifetimes of outflows estimated from CO observations. Hence, parsec-scale HH flows trace the mass loss behavior of a YSO for a significant fraction of its outflow phase.

Systematic trends in the properties of HH objects depend on the projected separation of the HH objects from their driving source. HH objects close to their sources often contain highly collimated, fast moving, but low excitation knots
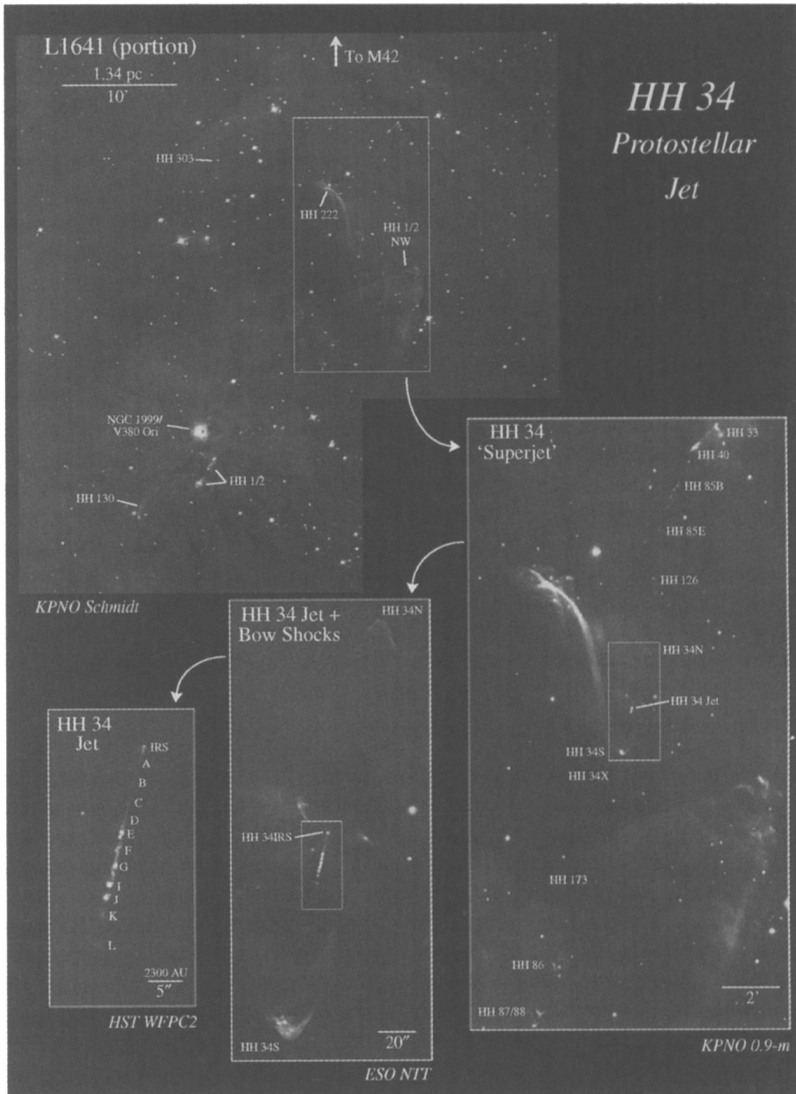
Figure 3.   Ground based and HST images of Hα+[S II] in the HH 34 system. A scale indicates the relative size of each frame. *Upper left.* KPNO 0.6 m Schmidt. *Lower right.* KPNO 0.9 m. *Lower middle.* ESO 3.5 m NTT *Lower left.* HST WFPC2

that trace the inner jet. Farther out, HH objects tend to be bow-shaped and exhibit higher excitation line emission. The most distant shocks appear highly fragmented with amorphous morphologies and have lower velocities than HH objects closer to the source. The sizes of HH objects increase with increasing distance from the driving source. Some HH shocks are nearly 1 parsec in extent (cf. the terminal bow shock of the HH 1/2 system; Ogura 1995)!

The observed properties of parsec-scale HH flows require several kinds of time-dependent mass-loss variability in the source. The periodicity, low excitation, and high proper motions of knots in the inner portion of the HH 34 jet can be explained by a *variable ejection velocity*, while the S-shaped symmetry seen in the extended HH 34 outflow complex and in PV-Cep can be explained by a *variable ejection angle*. The mass-loss rate and possibly the collimation angle may also be time-dependent.

Many parsec-scale HH flows are larger than their CO counterparts, which tend to have dimensions comparable to the host cloud cores (0.05 to 0.3 pc in CO). It is likely that close to their sources, jets entrain CO bearing gas and produce bipolar CO outflows, while farther from the source, they entrain predominantly atomic gas. Although high velocity "bullets" of CO have been detected beyond the confines of the HH 111 cloud core and its lower velocity CO outflow (Cernicharo & Reipurth 1996), the "bullets" likely contain ejected, rather than entrained, material.

Observations of parsec-scale flows can be used to constrain the mass ejection history of YSOs. The spacing of shocks increases with increasing distance from the source until, at more than several arcminutes away, they are well-separated shock systems. The gaps between the outermost shocks can be 10′ or greater. Preliminary analyses of well-studied systems suggest that mass-loss variability must be roughly distributed in time as a 1/f noise process (small-scale velocity variations occur with short time lags, while large-scale variations occur rarely and with large lags).

In several parsec-scale HH flows, shock-excited optical emission is seen towards low obscuration regions where galaxies and rich star fields are visible (cf. HH 111/311; L1551; L1228; PV-Cep). These outflows have punched out of their parent cloud cores and are pumping energy and momentum into the inter-clump medium (ICM) of GMCs or into the surrounding ISM. It is possible to constrain the nature of the ICM in GMCs by analysis of their terminal working surfaces.

The low extinction towards the lobes of several of the parsec-scale outflows and the large velocities observed for some flow components implies that UV and X-ray techniques may be used to investigate some outflows from young stars. It may be possible to detect highly ionized species, such as O VI, Si III, and C IV either in absorption against bright background stars or, in some cases, directly in emission.

The large number of known HH objects, their high surface area covering factor in active star forming regions, and their large angular scales imply that in regions such as NGC 1333 in Perseus and in many portions of Orion and other star forming regions, outflows profoundly effect the molecular cloud environment. Terminal working surfaces penetrate the cloud volume, blow-out of their host cores, shock, dissociate, and even ionize the material they encounter. Outflows may be important in the overall stability of clouds, their shocks may

dissociate molecules and be responsible for the large observed abundances of neutral or ionized carbon deduced from sub-mm and FIR observations, and may generate turbulence in molecular clouds.

References

Bally, J., Langer, W. D., & Liu 1991, ApJ, 383, 645

Bally, J., Langer, W. D., Stark, A. A., & Langer, W. D. 1987, ApJ, 313, L45

Bally, J., & Devine, D. 1994, ApJ, 428, L65

Chernin, L. M., & Masson, C. R. 1995, ApJ, 443, 181

Cernicharo, J., & Reipurth, B. 1996, ApJ, 460, 57

Fukui, Y., Iwata, T., Mizuno, A., Bally, J., & Lane, A. 1993, in *Protostars and Planets III*, ed.E. H. Levy & J. I. Lunine, U. of Arizona Press, p. 497

Ghosh, P., & Lamb, F. K. 1977, ApJ, 217, 578

Ghosh, P., & Lamb, F. K. 1978, ApJ, 223, L83

Herbig, G. H., & Terndrup, D. M. 1986, ApJ, 307, 609

Lada, C. J. 1985, *Ann. Rev. Astron. Astrophys.*, 23, 267

Lada, E. A., DePoy, D. L., Evans, N. J., & Gatley, I. 1991b, ApJ, 371, 171

Lada, E. A., Strom, K. M., & Myers, P. C. 1993 in *Protostars and Planets III*, ed.E. H. Levy & J. I. Lunine, U. of Arizona Press, p. 245

Lovelace, R. V. E., Romanova, M. M., & Bisnovatyi-Kogan, G. S., 1995, MNRAS, 275, 244

Masson, C. R., & Chernin, L. M. 1993, ApJ, 414, 230

McCaughrean, M. J., & Stauffer, J. R. 1994 AJ, 108, 1382

McCaughrean, M. J., & O'Dell, C. R. 1996, AJ, 111, 1977.

O'Dell, C. R., Wen, Z., & Hu, X. 1993, ApJ, 410, 696

O'Dell, C. R., & Wen, Z. 1994, ApJ, 436, 194

Ogura, K. 1995, ApJ, 450, L23

Ostriker, E. C., & Shu, F. 1995, ApJ, 447, 813

Raga, A. & Cabrit, S. 1993, A&A, 278, 267

Raymond, J. 1979, ApJS, 39, 1

Reipurth, B. 1983, A&A, 117, 183

Reipurth, B., Bally, J., Graham, J. A., Lane, A. P., & Zealey, W. J. 1986, A&A, 164, 51

Reipurth, B. 1994, A General Catalogue of Herbig-Haro Objects, electronically published via anon.ftp to ftp.hq.eso.org, directory /pub/Catalogs/Herbig-Haro

Reipurth, B., Bally, J., Devine, D. 1997, A&A(in press)

Schwartz, R. D. 1975 ApJ, 195, 631

Shu, F., Najita, J., Galli, D., Ostriker, E., & Lizano, S. 1993, in *Protostars and Planets III*, ed.E. H. Levy & J. I. Lunine, U. of Arizona Press, p. 3

Shu, F., Najita, J., Ostriker, E., Wilken, F., Ruden, S., & Lizano, S. 1994, ApJ, 429, 781

Stone, J. M., Xu, J., & Mundy, L. G. 1995, Nature, 377, 315

Wardle, M., & Konigl, A. 1993, ApJ, 410, 218

Discussion

M. Begelman: How tight are the angular collimations of the long jets, and how stable are the orientations of jet axes?

J. Bally: Opening angles range from under 1° for the most collimated jets (HH 333) to values around 3° to 6° for sources like HH 34, HH 111. The projected angular sizes of distant bow shocks correspond to somewhat wider opening angles of order $\sim 10°$ or more, suggesting that the larger outer shocks have spread ("splashed") orthogonal to the flow axis. Many (most?) parsec-scale jets show S-shaped symmetry that suggests precession on time scales ranging from 10^4 to 10^5 years.

J. Morse: Do the jets and disks observed in the Orion Nebula and the Orion molecular clouds show a preferred orientation, perhaps due to a large-scale magnetic field?

J. Bally: Neither the disks observed in the Orion Nebula region, nor the large-scale jets observed in the neighbouring molecular cloud cores, such as L1641, show evidence for any sort of coherent orientation. As far as we can tell from the HST data, the Orion Nebula disks appear to be oriented randomly.

H. Zinnecker: What is the estimated ratio between the overall radiated luminosity to mechanical luminosity in the jets that you have discussed (eg HH 34 and HH 111)? What fraction of the bolometric luminosity of the exciting jet energy source is involved?

J. Bally: For the youngest sources (Class 0), the mechanical luminosity of the jet (L_{mech}) is often comparable to the bolometric luminosity (L_{bol}) with $L_{mech} \sim (0.1-1)L_{bol}$. L_{mech} appears to decline as the source evolves to $\sim 10^{-2}-10^{-3}L_{bol}$ for the "classical" bipolar CO flows. However estimates of L_{mech} depend critically on estimates of $n(H)$, which are very uncertain due to the poor constraints of the ionisation function $n_e/n(H) \equiv X_e$ which can be much less than 1%. Observations usually constrain n_e through observations of the $\lambda 6717/\lambda 6731$ [S II] line ratio, and $n(H) \sim n_e/X_e$.